Quantifying flood-water impacts on a lake water budget via volume-dependent transient stable isotope mass balance

Janie Masse-Dufresne[1], Florent Barbecot[2], Paul Baudron[1,3] and John Gibson[4,5]

[1]Polytechnique Montréal, Department of Civil, Geological and Mining Engineering, Montreal, QC H3T 1J4, Canada
[2] Geotop-UQAM, Department of Earth and Atmospheric Sciences, Montreal, QC H2X 3Y7, Canada
[3] Institut de Recherche pour le Développement, UMR G-EAU, 34090 Montpellier, France
[4] Alberta Innovates Technology Futures, 3-4476 Markham Street, Victoria, BC V8Z 7X8, Canada
[5] University of Victoria, Department of Geography, Victoria, BC V8W 3R4, Canada

Correspondence to: Janie Masse-Dufresne (janie.masse-dufresne@polymtl.ca)

Abstract. Isotope mass balance models have undergone significant developments in the last decade, demonstrating their utility for assessing the spatial and temporal variability of hydrological processes, and revealing significant value for baseline assessment in remote and/or flood-affected settings where direct measurement of surface water fluxes to lakes (i.e., stream gauging) are difficult (or nearly impossible) to perform. The main objective of this study is to demonstrate quantitative application of an isotopic mass balance method to a flood-affected lake, which is then used to constrain water balance parameters and to gain insight into the dynamics of an important ungauged lake and its artificial recharge system used for local water supply. A volume-dependent transient isotopic mass balance model was developed for an artificial lake (named Lake A) in southern Quebec (Canada). This lake typically receives important flood-water inputs during the spring freshet period, as a perennial hydraulic connection with a large watershed is established each year. Quantification of the water fluxes to Lake A allow for impacts of flood-water inputs to be highlighted within the annual water budget. The isotopic mass balance model has revealed that groundwater and surface water inputs account for 71 % and 28 %, respectively, of the total annual water inputs to Lake A, which demonstrates an inherent dependence of the lake on groundwater. An important contribution to groundwater storage is likely related to flood-water recharge by the process of bank storage. On an annual timescale, Lake A was found to be highly sensitive to groundwater quantity and quality changes. However, it is likely that sensitivity to groundwater changes is lower from April to August, as important surface water inputs originating from Lake Deux-Montagnes (DM) contribute to the water balance via direct and indirect inputs (i.e., from bank storage). Our findings suggest not only that surface water fluxes between Lake DM and Lake A have an impact on the dynamics of Lake A during springtime, but significantly influence its long-term dynamics and help to inform, understand and predict future water quality variations. From a global perspective, this knowledge is useful for establishing regional-scale management strategies for maintaining water quality at flood-affected lakes, for predicting response of artificial recharge systems in such settings, and to mitigate impacts due to land-use and climate changes.

1 Introduction

Lakes are complex ecosystems which play valuable economic, social and environmental roles within watersheds (Kløve et al., 2011). In fact, lacustrine ecosystems can provide a number of benefits and services, such as biodiversity, water supply, recreation and tourism, fisheries and sequestration of nutrients (Schallenberg et al., 2013). The actual outcome of these ecosystem services often depends on the water quality of the lake (Mueller et al., 2016). Globally, the quantity and quality of groundwater and surface water resources are known to be affected by land-use (Lerner and Harris, 2009; Cunha et al., 2016; Scanlon et al., 2005) and climate changes (Delpla et al., 2009). As both surface water and groundwater contribute to lake water balances (Rosenberry et al., 2015), changes that affect the surface water/groundwater apportionment can potentially modify or threaten lake water quality (Jeppesen et al., 2014). Understanding the relative importance of the hydrological processes in lakes can also help to depict the vulnerability and/or resilience of a lake to pollution (Rosen, 2015) as well as to invasive species (Walsh et al., 2016) and thus secure water quantity and quality over time for drinking water production purposes (Herczeg et al., 2003). In Quebec (Canada), there are an important number of municipal wells that receive contributions from surface water resources (i.e., lakes or rivers) and are thus performing unintentional (Patenaude et al., 2020) or intentional (Masse-Dufresne et al., 2019; Masse-Dufresne et al., 2020) bank filtration.

Over the past few decades, significant developments have been made in application of isotope mass balance models for assessing the spatial and temporal variability of hydrological processes in lakes; most notably, the quantification of groundwater and evaporative fluxes (Herczeg et al., 2003; Bocanegra et al., 2013; Gibson et al., 2016; Arnoux et al., 2017a). Isotopic mass balance models are typically applied to contexts where there are no surface water inputs (Sacks et al., 2014; Arnoux et al., 2017b) and/or the surface water inputs are quantified by stream gauging (Stets et al., 2010). In remote environments, such as in northern Canada, application of isotopic methods is particularly convenient, as direct measurement of surface water inflow is difficult or nearly impossible (Turner et al., 2010; Brock et al., 2007). Recently, Haig et al. (2020) opened up new perspectives, as they reported excellent agreement between results obtained via isotopic mass balance and gauging techniques when assessing the water budget of connected lakes in Saskatchewan (Canada). They highlighted that the isotopic approach was efficient for characterizing the impacts of floods and droughts, and that a broad application can contribute to water resources management in providing information to understand the vulnerability of ungauged systems. As future climate change impacts are expected to include increases in flood magnitude and frequency (Aissia et al., 2012), flood-affected lake water budget assessments are of utmost importance.

The main objective of this study is to demonstrate the application of isotopic mass balance to flood-affected lakes, as this approach is particularly opportune in providing estimates of the water balances and insights on the dynamics of ungauged systems. We thus evaluate the importance of flood-water inputs (and bank storage) on the annual water budget of a lake located in a floodplain in an urban area, in order to depict its resilience to changes in water balance partitioning and flood-water and/or groundwater quality. To do so, we first aim to establish an isotopic framework based on the local water cycle, to verify the applicability of isotopic mass balance in the present setting, as contrasting isotopic signatures are required between various water storages and fluxes, including flood-water inputs. Secondly, we quantify the water budget according to two reference scenarios (A and B) to grasp the impact of site-specific uncertainties on the computed results. Then, we analyze the temporal variability of the groundwater inputs and the sensitivity of the lake to flood-water driven pollution. Finally, we demonstrate the implications of flood-water storage on the water balance partition. It is hypothesized that the groundwater fluxes (inputs and outputs) through lake banks are unneglectable in lake water budgets, even for flood-affected lakes.

The water balance is computed via a volume-dependent transient isotopic mass balance model, which is applied to predict the daily isotopic response of an artificial lake in Canada that is ephemerally connected to a 150,000 km^2 watershed during spring freshet and other periods of flooding. During these recurring perennial flood events, the surficial water fluxes entering the study lake are not constrained in a gaugeable river or canal but occur over a 1-km wide surficial flood area. Our study period spans a 100-year flood, and the results of this study are therefore an example indicative of an extreme hydrological event.

A previous study by Zimmermann (1979) similarly used a transient isotope balance to estimate groundwater inflow and outflow, evaporation, and residence times for two young artificial groundwater lakes near Heidelberg, Germany, although these lakes had no surface water connections, and volumetric changes were considered negligible. Zimmermann (1979) showed that the lakes were actively exchanging with groundwater, which controlled the long-term rate of isotopic enrichment to isotopic steady state, but the lakes also responded to seasonal cycling in the magnitude of water balance processes. While informative, Zimmermann (1979) did not attempt to build a predictive isotope mass balance model, but rather used a best-fit approach to obtain a solitary long-term estimate of water balance partitioning for each lake. Petermann et al. (2018) also constrained groundwater connectivity for an artificial lake near Leipzig, Germany, with no surface inlet nor outlet. By comparing groundwater inflow rates obtained via stable isotope and radon mass balances on a monthly time-step, Petermann et al. (2018) highlighted the need to consider seasonal variability when conducting lake water budget studies. Our approach builds on that of Zimmermann (1979) and Petermann et al. (2018), developing a predictive model of both atmospheric and water balance controls on isotopic enrichment, and accounting for volumetric changes on a daily time step.

2 Study site

2.1 Geological and hydrological settings

Located in southern Quebec, Canada, Lake A is a small artificial lake created by sand dredging activities with a maximum observed depth of 20 m (Fig. 1a). The lake constitutes the main water resource for a bank filtration system (Masse-Dufresne et al., 2019) which is designed to supply drinking water for up to 18000 people (Ageos, 2010). The lake volume (4.70 x 10^6 m^3) was estimated based on its surface area (2.79 x 10^5 m^2 in October 2016, measured on *Google Earth Pro*), maximum observed depth, and assuming lake bank slopes of 25 degrees (Holtz and Kovacs, 1981). An assessment of the impact of uncertainty regarding the lake geometry on the model calculation is provided in Sect. 4.3.2. The lake was excavated within alluvial sands which were deposited in a paleo valley carved into the Champlain Sea Clays (Ageos, 2010). Lake A receives inflow from a small stream (S1) with a mean and maximum annual discharge of 0.32 $m^3 s^{-1}$ and 1.19 $m^3 s^{-1}$, respectively. Maximum discharge typically occurs during the month of April as S1 drains snowmelt water from a small watershed (14.4 km^2) (Centre d'Expertise Hydrique du Québec, 2019), whereas low to no flow is recorded for the rest of the hydrological year.

Two channelized outlet streams (S2 and S3) allow water to exit Lake A and flow towards Lake Deux-Montagnes (DM). The flow direction at S2 and S3 can be temporally reversed (Fig. 1b) when the water level of Lake DM is above the topographic threshold of 22.12 m.a.s.l. (Ageos, 2010). This process typically occurs during springtime (from April to May) and, to a lesser extent, during autumn (from October to December) and results in the inundation of the area between Lake A and Lake DM. Thus, during these flood events, the surficial water fluxes towards Lake A are not constrained in S2 and S3 but occur over a 1 km wide area. While alluvial sands were mapped in the area between Lake A and Lake DM (Fig. 1b), stratigraphic data (i.e., well logs) confirms that only a thin layer (few centimeters to roughly 2 meters) of alluvial sands are deposited on top the clayey sediments in the area between Lake A and Lake DM (see Fig. 1c). Hence, it is likely that little or no subsurface hydraulic connection exists between Lake A and Lake DM.

Significantly, Lake DM is the receiving waters for the Ottawa River, which drains a large watershed of approximately 150000 km^2 (MDDELCC, 2015) and in turn drains to the St. Lawrence River (Fig. 1a), which is an important drinking water supply for the Cities of Montreal and Quebec.

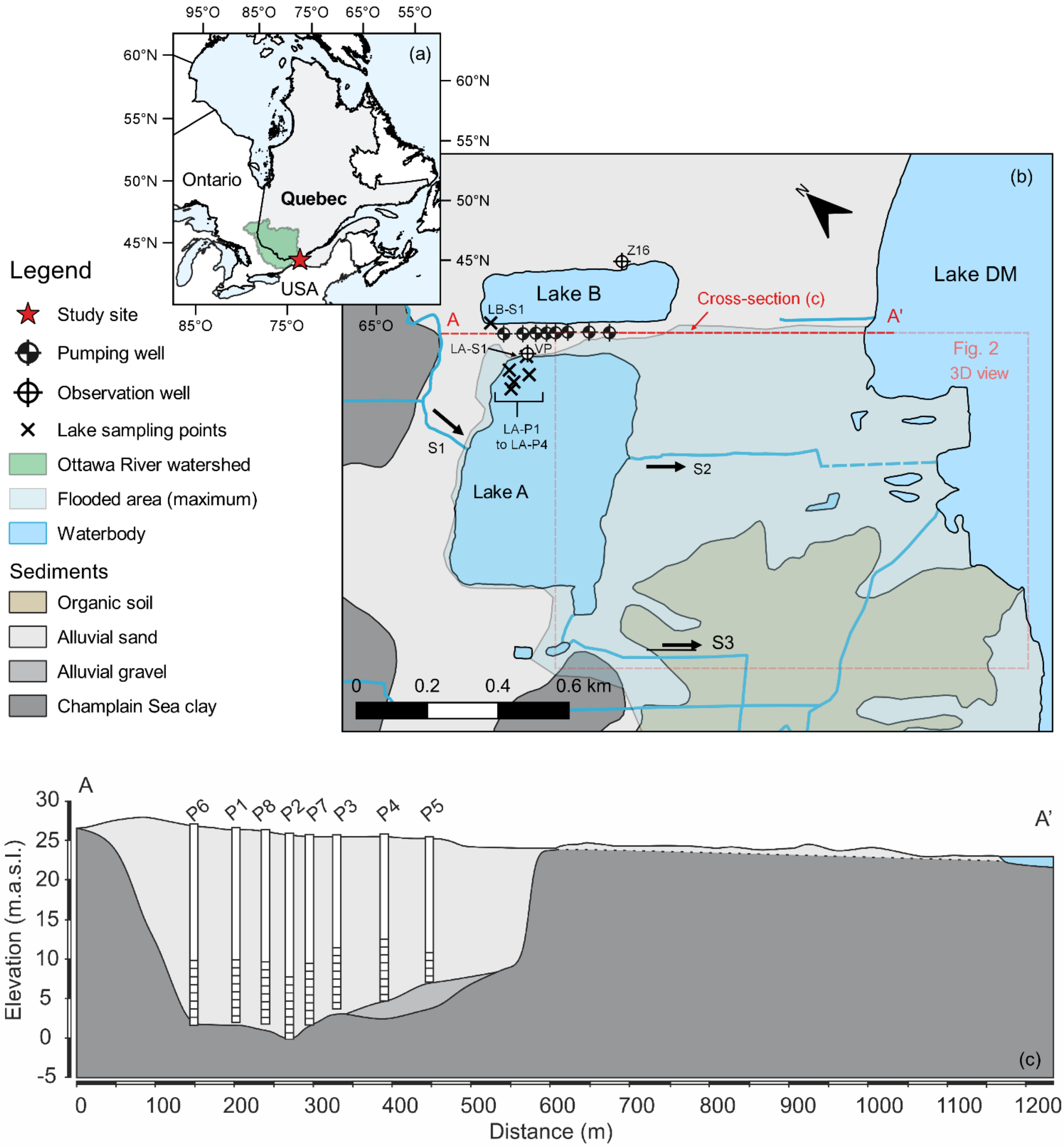

Figure 1. (a) Location of the study site and Ottawa River watershed, (b) schematic representation of the hydrogeological context and location the lakes and monitoring and sampling points, and (c) geological A-A' cross-section showing the buried valley carved into the Champlain Sea clays and filled with alluvial gravels and sands. LA-S1 and LB-S1 are surface water sampling points at Lake A and Lake B, respectively. LA-P1 to LA-P4 correspond to vertical profile sampling locations at Lake A. Monitoring of the water levels was conducted observation well VP. The maps were created based on open access Geographic Information System (GIS) data. Canada's provinces boundary files were obtained from Statistics Canada © and USA Cartographic Boundary Files were retrieved from the United States Census Bureau ©. Hydrological data (lakes, streams and watershed) was sourced from the Nation Hydro Network – NHN – GeoBase Series and provided by the Strategic Policy and Results Sector of Natural Resources Canada ©. The flood extent products are derived from RADARSAT-2 images with a system developed and operated by the Strategic Policy and Results Sector of Natural Resources Canada ©. The surface sediments data correspond to "Géologie du quaternaire - Jeux de données géographiques – Zones morphosédimentologiques" and are available from Ministère de l'Énergie et des Ressources naturelles; Secteur de l'énergie et des mines – Direction de l'information géologique du Québec ©.

2.2 Conceptualization of the groundwater-surface water interactions

Based on the geological and hydrological context of the study site, we established a conceptual model of the groundwater-surface water interactions (Fig. 2) divided in two distinct hydrological periods: (i) the flood-water input periods and (ii) the normal periods.

During the flood-water input period, we hypothesize that the surface water inputs (I_S) and precipitations (P) represent the total water inputs to Lake A (Fig. 2a). High-water levels at Lake A impose a hydraulic gradient at the lake-aquifer interface which inhibits groundwater inflows (I_G). Contrastingly, it is assumed that I_G constitutes the main water input to Lake A during the normal periods, while I_S is neglectable (Fig. 2b). In fact, as the flood-water inputs stop, the water level at Lake A lowers and the hydraulic gradient at the lake-aquifer interface is reversed and allows for I_G to flow to the lake. For both periods, the outputs are occurring through evaporative fluxes (E), surface water outflows (Q_S) and groundwater outflows (Q_G).

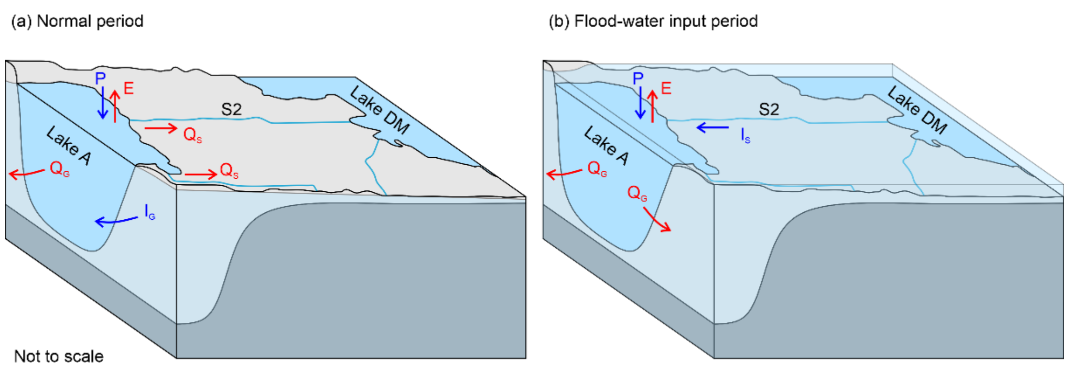

Figure 2. Schematic representation of the hydrological processes at Lake A during (a) normal periods, and (b) flood-water input periods. Inputs include precipitation (P), surface water (I_S) and groundwater (I_G) while outputs include evaporation (E), surface water outflow (Q_S) and groundwater outflow (Q_G). The area between Lake DM and Lake A is flooded in (b) and I_S from Lake DM contribute to the water balance of Lake A.

3 Methods

3.1 Field measurements

Level loggers (Divers®; TD-Diver and CTD-Diver) were used to measure water levels at Lake A and observation well VP. Water levels were recorded with a 15-minute time step starting on April 17, 2017 (after the ice-cover melted) and March 29, 2017 at Lake A and VP, respectively. All the level loggers' clocks were synchronized with the computer's clock when launching automatic measurements for a 3-month period. This procedure was done via the Diver-Office 2018.2 software. Manual measurements of the water level were regularly performed to calibrate (relatively to a reference datum) and validate the automatic water level measurements. Mean daily water levels at Lake DM were retrieved with permission from the *Centre d'Expertise Hydrique du Quebec* database (Centre d'Expertise Hydrique du Québec, 2020). Meteorological data from Mirabel International Airport station (45.68 °N, -74.04 °E) were used for further computations and were retrieved from Environment and Climate Change Canada database (available online at weatherstats.ca). Daily precipitation and solar radiation data were retrieved from two nearby stations, namely Sainte-Anne-de-Bellevue (45.43 °N, -73.93 °E) and Montreal International Airport (45.47 °N, -73.75 °E), as these parameters were not available at the closest station.

3.2 Water sampling and analytical techniques

Water sampling and physico-chemical parameters (including temperature, electrical conductivity, pH and redox potential), and in-situ measurements were performed at Lake A close to the surface near the lake edge on a weekly to monthly basis. Physico-chemical parameters were measured using a multiparameter probe (YSI Pro Plus 6051030 and Pro Series pH/ORP/ISE and Conductivity Field Cable 6051030-1, YSI Incorporated, Yellow Springs, OH, USA). Additional field campaigns were conducted on February 9, 2017, August 17, 2017 and January 25, 2018 in order to perform vertical profile measurements and water sampling at various depths (e.g. 2 m, 4 m, 8 m, 12 m and 15 m) at LA-P1 to LA-P4. Lake water sampling was performed in the northern part of the lake for logistical reasons and due to ease of accessibility. As horizontal homogeneity has been previously demonstrated by Pazouki et al. (2016), the water samples were deemed representative of the whole waterbody.

Flood water was sampled at two locations (near S2 and S3) on April 19, 2017 and at Lake DM on May 10, 2017. Water samples were also collected at the surface and at depth within Lake B and at observation well Z16, which is upstream of Lake B and, thus, representative of the regional groundwater contributing to the latter (Ageos, 2016).

Water samples were analyzed for major ions, alkalinity and stable isotopic compositions of water ($\delta^{18}O$ and $\delta^{2}H$). Water was filtered in the field using 0.45 µm hydrophilic polyvinylidene fluoride (PVDF) membranes (Millex-HV, Millipore, Burlington, MA, USA) prior to sampling for major ions and alkalinity. From December to March, cold weather prevented field filtration, so this procedure was performed in the laboratory on the same day. All samples were collected in 50-ml polypropylene containers and kept refrigerated at 4 °C during transport and until analysis, except for stable isotopes, which were stored at room temperature. Major ions were analyzed within 48 h via ionic chromatography (ICS 5000 AS-DP Dionex Thermo Fisher Scientific, Saint-Laurent, QC, Canada) at Polytechnique Montreal (Montreal, Quebec). The limit of detection was ≤0.2 mg/L for all major ions. Bicarbonate concentrations were derived from alkalinity, which was measured manually in the laboratory according to the Gran method (Gran, 1952) at Polytechnique Montreal (Montreal, Quebec). On samples with measured alkalinity (n = 12), the ionic balance errors were all below 8%. The mean and median ionic balance errors were 1%. Stable isotopes of oxygen and hydrogen were measured with a Water Isotope Analyser with off-axis integrated cavity output spectroscopy (LGR-T-LWIA-45-EP, Los Gatos Research, San Jose, CA, USA) at Geotop-UQAM (Montreal, Quebec). 1 ml of water was pipetted in a 2 ml vial and closed with a septum cap. Each sample was injected (1 microliter) and measured 10 times. The first two injections of each sample were rejected to limit memory effects. Three internal reference waters ($\delta^{18}O$ = 0.23±0.06‰, -13.74±0.07‰ & -20.35±0.10‰; $\delta^{2}H$ = 1.28±0.27‰, -98.89±1.12‰ & -155.66±0.69‰; $\delta^{17}O$ = 0.03±0.04‰, -7.32±0.06‰ & -10.80±0.06‰) were used to normalize the results on the VSMOW-SLAP scale. A 4th reference water ($\delta^{18}O$ = -4.31±0.08‰; $\delta^{2}H$ = -25.19±0.83‰; $\delta^{17}O$ = -2.31±0.04‰) was analyzed as an unknown to assess the exactness of the normalization. The overall analytical uncertainty (1 σ) is better than ±0.1‰ for $\delta^{18}O$, ±1.0 ‰ for $\delta^{2}H$ and

±0.1‰ for $\delta^{17}O$. This uncertainty is based on the long-term measurement of the 4th reference water and does not include the homogeneity nor the representativity of the sample (Light stable isotope geochemistry laboratory of Geotop-Uqam).

3.3 Stable isotope mass balance

Stable isotope mass balances can either be performed based on (i) a well-mixed single layer model or (ii) a depth resolved multi-layered model. In a recent study, Arnoux et al. (2017b) compared a well-mixed model and a depth-resolved multi-layer model. Both models yielded similar results and provided a general understanding of the groundwater-surface water interactions. The multi-layer model additionally allowed for the determination of groundwater flow with depth, but required a temporally- and depth-resolved sampling in order to ensure a thorough understanding of the stability/mixing of the different layers. Such important sampling and monitoring efforts are however often unrealistic in remote and/or flood-affected contexts. Additionally, Gibson et al. (2017) studied the impact of sampling strategies on the water yield (i.e., the depth-equivalent runoff to the lake) estimations for the Turkey Lake (32 m deep) under stratified and well-mixed conditions. They reported 18% difference on the water yield when performing grab sampling (i.e., 1 sample at 1 m depth) and bulk sampling (i.e., assessment of the whole lake water column). The difference was less important (i.e., 11%) when comparing bulk sampling to integrated sampling for epilimnion, metalimnion and hypolimnion. They also reported discrepancies up to 20% for the water yield estimations at the same lake according to the timing of the lake water sampling. This last result shows that temporal shifts may induce greater bias than the uncertainty related to the lake stratification. For these reasons, we advocated the application of a well-mixed model.

The water and stable isotope mass balance of a well-mixed lake can be described, respectively as Eq. (1) and Eq. (2):

$$\frac{dV}{dt} = I - E - Q \quad (1)$$

$$V\frac{d\delta_L}{dt} + \delta_L\frac{dV}{dt} = I\delta_I - E\delta_E - Q\delta_Q \quad (2)$$

where V is the lake volume, t is time, I is the instantaneous inflow, E is evaporation, Q is the instantaneous outflow. I correspond to the sum of surface water inflow (I_S), groundwater inflow (I_G) and precipitations (P). Similarly, Q is the sum of surface water outflow (Q_S) and groundwater outflow (Q_G). δ_L, δ_I, δ_E and δ_Q are the isotopic compositions of the lake, the inflow, evaporative and outflow fluxes, respectively. The application of Eq. (1) and Eq. (2) for both $\delta^{18}O$ and δ^2H is valid during the ice-free period and also assumes constant density of water (Gibson, 2002). In this study, the potential impacts of the ice-cover formation and melting are neglected, as the ice volume is likely to represent only a small fraction (<2%) of the entire water body. Moreover, considering the ice-water isotopic separation factor, i.e., 3.1 ‰ for $\delta^{18}O$ and 19.3 ‰ for δ^2H (O'Neil, 1968) and assuming well-mixed conditions, the lake water isotopic variation would be comprised within the analytical uncertainty. Also, flood-water inputs from Lake DM were expected to be much more important and occurring simultaneously with ice-melt during the freshet period.

Thus, a volume-dependent model is applied, as described in Gibson (2002). The change in the isotopic composition of the lake (δ_L) with f (i.e., the remaining fraction of lake water) can be expressed as Eq. (3):

$$\delta_L(f) = \delta_S - (\delta_S - \delta_0) f^{\left[\frac{-(1+mX)}{1-X-Y}\right]} \quad (3)$$

where X = E/I is the fraction of lake water lost by evaporation, Y=Q/I is the fraction of lake water lost to liquid outflows, m is the temporal enrichment slope (see Appendix A), and δ_S is the steady-state isotopic composition the lake would attain if f tends to 0 (see Appendix A).

A step-wise approach is used to solve Eq. 3 on a daily time-step. At each time step, recalculation of $f=V/V_0$ is needed, where V is the residual volume at the end of the time step and V_0 the original volume at the beginning of the time step (or V^{t-dt}). Hence, Eq. (3) is based on the water level difference between two days.

The water fluxes parameters (E, I and Q) and isotopic signatures (δ_E, δ_A, δ_I and δ_Q) are thus evaluated on a daily time-step.

3.4 Water fluxes

Evaporative fluxes (E) are calculated using the Penman evaporation equation, as described in Valiantzas (2006):

$$E_{Penman-48} = \frac{\Delta}{\Delta+\gamma} \cdot \frac{R_n}{\lambda} + \frac{\gamma}{\Delta+\gamma} \cdot \frac{6.43 f(u) D}{\lambda} \quad (4)$$

where R_n is the net solar radiation (MJ m^{-2} d^{-1}), Δ is the slope of the saturation vapor pressure curve (kPa °C^{-1}), γ is the psychrometric coefficient (kPa °C^{-1}), λ is the latent heat of vaporization (MJ kg^{-1}), *f*(*u*) is the wind function (see Appendix A) and D is the vapor pressure deficit. For comparative purposes, estimation of the daily evaporative fluxes was also conducted with the Linacre-OW equation (Linacre, 1977) and the open-water simplified version of Penman-48 (Valiantzas, 2006).These methods yielded similar evaporation estimates from April to August but underestimated total evaporation by 24 % to 33 % compared to the Penman-48 equation. The discrepancy between the models is restricted to late summer and autumn (see Appendix B, Fig. B1) and is attributed to the difference between the air and water surface temperature, which was estimated based on the equilibrium method as described by de Bruin (1982) (see Appendix C). Note that E and P are set to zero during the ice-cover period (i.e. from January 1st to March 31, based on meteorological data and field observations).

For well-mixed conditions, the δ_{Qs} and δ_{Qg} are assumed to be equal to δ_L. Hence, no separation of these two fluxes is attempted and they are merged into one variable, i.e., the non-fractionating outflow (Q). Outflow was adjusted to obtain the best fit between the observed and modelled values. The direction and intensity of the water flux at the lake-aquifer interface can be conceptually described by Darcy's Law. The outflows from the lake are thus roughly proportional to the lake water level, as the variation of the cross-sectional area is negligible, given the significant depth of Lake A (i.e., 20 m) in comparison to the maximum water level change during the flooding event (i.e., 2.7 m). Considering the above, it was assumed that the daily outflow flux from Lake A varied linearly according to the lake water level; the minimum and maximum outflow (Q_{min} and Q_{max}) corresponding to the minimum and maximum water level, respectively. The outflow range (i.e., minimum and maximum values) was adjusted to obtain best fit between the calculated and observed δ_L.

Total daily inflow (sum of daily P, I_s and I_G) into Lake A compensates for the adjusted daily outflow and daily lake volume difference. The precipitations (P) are evaluated from the available meteorological data (see Sect. 3.1), while direct measurement of I_S and I_G was not possible in this hydrogeological context (see Sect. 2.1). Consequently, further assumptions are needed to apportion these contributions. Considering the proposed conceptual model of the groundwater-surface water interactions (see Sect. 2.2), I_S is set to zero, while I_G is contributing to the lake during normal periods. On the other hand, during the flood-water input period (i.e., from February 23, 2017 to May 8, 2017), the rising water level at Lake A results in a hydraulic gradient forcing the lake water to infiltrate the aquifer and inhibiting I_G. It is assumed that I_S originate exclusively from Lake DM. Potential surface water inflow from S1 and runoff are not evaluated, as the isotopic composition of S1 is expected to be similar to the flood-water inputs. Moreover, as explained in Sect.2.1, important flow is only observed at S1 during springtime, while negligible or no flow is observed otherwise. Hence, these potential inputs are comprised within the I_S.

4 Results

4.1 Hydrodynamics of the flood event

Water level of Lake DM typically rises during springtime due to precipitation and/or snowpack melting over the Ottawa River watershed (Centre d'Expertise Hydrique du Québec, 2020) and results in a yearly recurrent flooding of Lake A. The temporal evolution of the mean daily water level at Lake DM, Lake A and observation well VP from February 2017 to January 2018 is depicted in Fig. 2.

During springtime 2017, rapid water level rises at Lake DM occurred in late February, early April and early May at rates of approximately 0.11 m d^{-1}, 0.19 m d^{-1} and 0.16 m d^{-1}, respectively. A historical maximum water level (i.e., 24.77 m.a.s.l.) was reached on May 8, 2017, resulting in a net water level rise of >2.7 m (compared to early February).

The water level variations at Lake A and observation well VP are synchronous with those of Lake DM (Fig. 3) from late February to late July 2017. Moreover, the water levels of Lake DM and Lake A were almost equal, and the daily variations were very similar for the observed period. Considering this, and a visible hydraulic connection between the water bodies, it becomes clear that Lake DM was controlling the surface water level of Lake A and, consequently, the water table elevation at observation well VP during this period. Indeed, the elevation of the natural threshold (i.e., 22.12 m.a.s.l.) was exceeded by Lake DM from February 23, 2017 to late July 2017, allowing surface water exchanges between Lake DM and Lake A.

Then, from August to late October, the water level at Lake DM is below the topographical threshold, and there is no similarity between the evolution of the water level at Lake DM and observation well VP. Hydraulic connection between Lake DM and Lake A established again in November, and the evolution of Lake DM and VP is more similar.

Note that water levels in Lake A were not continuously recorded after June 3, 2017 due to a logger failure, but manual water level measurements (in September 2017, December 2017 and January 2018) depict the general evolution of Lake A water level.

From February 23, 2017 to May 8, 2017, the relative volume of Lake A is globally increasing, and the net water fluxes are mainly positive (see shaded area in Fig. 3). The maximum volume change of Lake A was 7.6 x 10^5 m^3, which represents 16 % of the lake's initial volume. The maximum net water flux was 1.2 x 10^5 m^3 d^{-1}, corresponding to a water level rise of 0.43 m (on April 5, 2017 only). From May 9, 2017 to mid-August 2017, Lake A volume was decreasing, and the daily net water fluxes were mainly negative. In early August 2017, Lake A regained its initial volume. Then, in autumn and winter, the volume of Lake A was oscillating, and the net water fluxes were ranging from -6.4 x 10^4 m^3 d^{-1} to 5.3 x 10^4 m^3 d^{-1}. At the end of the study period (i.e., on January 25, 2018), a net volume difference of 1.5 x 10^5 m^3 remained at Lake A compared to February 9, 2017. However, the evolution of Lake A volume and the net water fluxes are not representative of the surface water/groundwater interactions. As dredged lakes are known to be hydraulically connected with groundwater (Zimmermann, 1979), the total outflows from Lake A during springtime are likely to be much more important than the net water fluxes.

For that reason, the development of a volume-dependent transient stable isotope mass balance was required to correctly depict the importance of the flood-water inputs on the water mass balance of the lake.

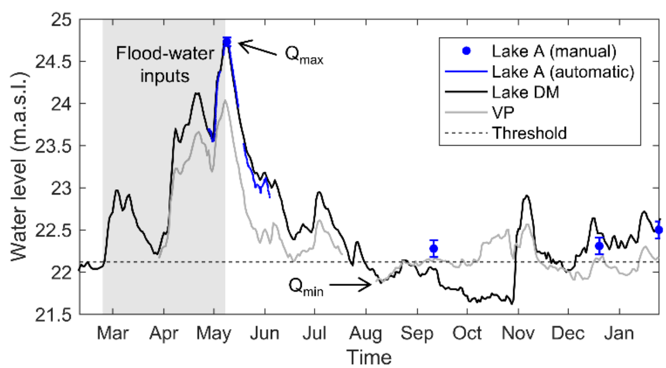

Figure 3. Daily mean water levels at Lake DM, Lake A and observation well VP from February 9, 2017 to January 25, 2018. The grey shaded area corresponds to the flood-water input period.

4.2 Isotopic and geochemical framework

The isotopic composition of precipitation (δ_P), Lake A and flood-water are depicted in Fig. 4. The Local Meteoric Water Line (LMWL) was defined using an ordinary least squares regression (Hughes and Crawford, 2012) using isotope data in precipitation from St-Bruno station IRRES database (*n* = 27; from December 2015 to June 2017).

For the study period, the isotopic composition of bulk precipitation was available on a biweekly to monthly time-step (*n* = 15) and ranged from -19.19‰ to -6.85‰ for $\delta^{18}O$ and -144‰ to -38‰ for δ^2H. Interpolation was used to simulate the δ_P on a daily-time step for the isotope mass balance model computation. The regional amount-weighted mean δ_P is -10.2‰ for $\delta^{18}O$ and -68‰ for δ^2H (calculated from the IRRES database for the year 2016). The latter compares well with the GNIP database long-term Ottawa amount-weighted mean (-10.9‰ for $\delta^{18}O$ and -75‰ for δ^2H) (IAEA/WMO, 2018).

Isotopic compositions of Lake A water samples (n = 39) are linearly correlated (see solid blue line) and all plot below the Local Meteoric Water Line (LMWL), which confirms that Lake A is influenced by evaporation. Linear regression of Lake A water samples defines the Local Evaporation Line (LEL), which is $\delta^2H = 5.68 (\pm 0.27) * \delta^{18}O - 12.80 (\pm 2.83)$ ($R^2 = 0.92$). Some samples from the surface of Lake A plot below the LEL, likely indicating snowmelt water inputs as noted in previous studies of Canadian lakes (Wolfe et al., 2007).

The isotopic composition of the flood-water samples (n = 3) is indeed more depleted than Lake A waters (i.e. $\delta^{18}O$ from -11.85 ‰ to -11.18 ‰ and δ^2H from -81 ‰ to -78 ‰) and is most likely to reflect the significant contribution from heavy isotope depleted snowmelt waters. The flood-water samples are also linearly correlated and plot along a line ($\delta^2H = 5.33\ \delta^{18}O - 18.82$) which slope is similar to Lake A LEL, suggesting that the sampled flood water evaporated under same conditions as Lake A water samples. For simplification purpose, the isotopic composition of the surface water inflow (δ_{Is}) was set to the intersection between the flood-water LEL and the LMWL($\delta^{18}O$ = -12.00 ‰ and δ^2H = -83 ‰). Similar isotopic compositions were recorded upstream of Lake DM during the snowmelt period near our study site (i.e., 34 km upstream in the watershed) from 1998 to 2009 (Rosa et al., 2016).

It has been argued that the LMWL-LEL intersection is representative of the isotopic composition of the inflowing water to a lake and is thus commonly used to depict the isotopic signature of groundwater (δ_G) in isotopic mass balance applications (Gibson et al., 1993; Wolfe et al., 2007; Edwards et al., 2004). Concerning the study site, the intersection between the St-Bruno LMWL and Lake A LEL corresponds to -11.26 ‰ for $\delta^{18}O$ and -77 ‰ for δ^2H. It was used as an estimate of δ_G in the isotopic mass balance model. It is noteworthy that estimating the δ_G from direct sampling at observation wells in the vicinity of lakes may be misleading due to potential heterogeneity (i.e., mixing between groundwater and surface water in the hyporheic zones). This consideration is particularly important at flood-affected lakes, as surface water-groundwater interactions are expected. In this context, it is advocated to estimate δ_G from the LMWL-LEL as it better represents the inflowing water to a lake.

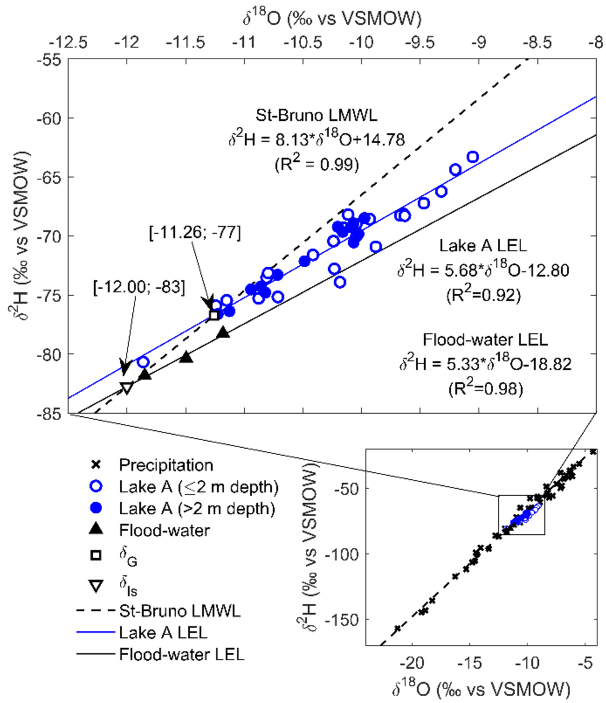

Figure 4. Isotopic composition of precipitation, Lake A water, and flood-water from March 2017 to January 2018. Hollow and solid blue circles correspond to samples collected at ≤2 m and >2 m depth, respectively. Analytical precision is 0.15‰ and 1‰ at 1σ for $\delta^{18}O$ and $\delta^{2}H$. Precipitation data are retrieved from the research infrastructure on groundwater recharge database (Barbecot et al., 2019).

The geochemical facies of Lake A and Lake DM samples are illustrated in Fig. 5 by the means of a Piper diagram. Mean values for Lake B and regional groundwater (GW) geochemical facies are also plotted for comparison purpose. Both Lake A and flood-water were found to be Ca-HCO_3 types, which is typical for precipitation- and snowmelt-dominated waters (Clark, 2015). The geochemistry of Lake A is relatively constant throughout the year and reveals a depth-wise homogeneity. The geochemistry of Lake B is significantly distinct from Lake A and appears to be influenced by a regional groundwater characterized by a Na-Cl water type.

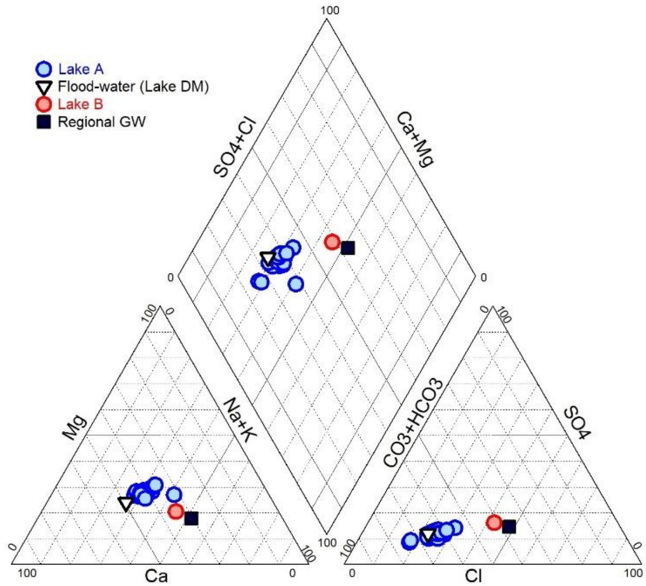

Figure 5. Geochemical facies of Lake A (*n* = 23) and flood-water (*n* = 1). Mean values for Lake B (*n* = 42) and regional groundwater (GW) (*n* = 11) geochemical facies are also plotted. Lake A and flood-water are characterized by Ca-HCO3 water types, while Lake B and regional GW correspond to Na-Cl water types. Note that regional GW was sampled upstream of Lake B.

4.3 Evaluation of the water budget

4.3.1 Volume dependent isotopic mass balance model

As described in Sect. 3.3, the isotopic mass balance model was solved iteratively by recalculating δ_L on a daily time-step. This model was developed assuming (1) well-mixed conditions and (2) that the outflow fluxes are proportional to the lake's water level. We adjusted minimum and maximum outflow fluxes (Q_{min} and Q_{max}) so that the latter respectively correspond to the minimum and maximum water levels (see Fig. 3). Lake A volume variations are estimated from water level records at Lake A and assuming a constant lake area. When not available, water levels at Lake DM or observation well VP are used as proxies. Water level of Lake DM is used when there is a hydraulic connection with Lake A (i.e., above the topographical threshold) and data from observation well VP is used otherwise. These approximations were deemed acceptable because the simulation of δ_L depends on the remaining fraction of lake water (not the absolute water level), and daily variations of the water levels at Lake A, Lake DM and observation well VP were shown to be similar (see Sect. 4.1).

Three sampling campaigns (i.e., on February 9, 2017, August 17, 2017 and January 25, 2018) were conducted at Lake A in order to collect water samples for isotopic analyses from the epilimnion, metalimnion and hypolimnion (Fig. 6) to account for the vertical stratification of the isotopic signature (Gibson et al., 2017). The isotope vertical profiles were volume-weighted according to the representative layer for each discrete measurement in order to obtain the observed δ_L for each campaign (Table

1). The depth-averaged isotopic composition of the lake on February 9, 2017 (i.e., $\delta^{18}O$ = -10.15 ‰ and $\delta^{2}H$ = -70 ‰) was used as the initial modelled δ_L.

Table 1. Observed depth-averaged (or mean) and standard deviation (std) of isotopic composition of Lake A for the sampling campaigns in February 2017, August 2017 and January 2018 and all samples.

Date	**$\delta^{18}O$ (‰)**		**$\delta^{2}H$ (‰)**	
	depth-averaged	**std**	**depth-averaged**	**std**
Feb 9, 2017	-10.15	0.11	-69.92	0.41
Aug 17, 2017	-10.61	0.82	-73.33	4.41
Jan 25, 2018	-10.70	0.26	-73.70	1.22
All samples (from Feb 9, 2017 to Jan 25, 2018)	-10.32*	0.62	-71.35*	3.69

* mean

While depth-average δ_L was not available at the end of the flood-water input period (i.e., in early May), water samples from the surface of Lake A provide relevant evidences to better constrain the model. Two scenarios, namely A and B, were considered. Until early May, the observed surface water temperature was < 5°C (see Fig. C1), which translates to a limited density gradient along the water column and does not allow for the development of a thermal stratification. In this context, it is possible to assume that Lake A is fully mixed until early May and that the water samples from the surface of the lake are representative of the whole water body. Hence, the modeled δ_L is additionally constrained at $\delta^{18}O \approx -11.1$‰ and $\delta^{2}H \approx -77$‰ (in early May) and at $\delta^{18}O \approx -11.6$‰ and $\delta^{2}H \approx -80$‰ (in late April) for scenarios A and B, respectively.

The results of the volume-dependent isotopic mass balance for $\delta^{18}O$ and $\delta^{2}H$ are illustrated in Fig. 6. The fitted Q_{min} and Q_{max} from Lake A are 3.7 x 10^4 m^3 d^{-1} and 8.0 x 10^4 m^3 d^{-1} and 1.0 x 10^3 m^3 d^{-1} and 2.8 x 10^5 m^3 d^{-1} and representing equivalent water level variations of 0.13 m d^{-1} and 0.29 m d^{-1} and 0.004 m d^{-1} and 1.0 m d^{-1} for scenario A and B respectively. From February 23, 2017 to May 8, 2017 (see grey shaded area), hydraulic conditions allowed for surface inputs (I_s) from Lake DM to Lake A at a mean rate of 6.61 x 10^4 m^3 d^{-1} with a total flood-water volume of 4.82 x 10^6 m^3 for the scenario A. The total flood-water volume was twice as important (9.96 x 10^6 m^3) for the scenario B. Then, from May 9, 2017, we considered that these flood-water inputs stopped, as the lake water level started to decrease. As a consequence, the model yielded a gradual enrichment of δ_L due to the combined contribution from I_G and E for both scenarios. From May 9, 2017 to January 25, 2018, the total I_G were 1.16 x 10^7 m^3 and 1.48 x 10^7 m^3 for scenario A and B respectively. Overall, the $\delta^{18}O$ and $\delta^{2}H$ models were better at reproducing the January 2018 and August 2017 observed δ_L, respectively. This is likely linked to the uncertainties and representativeness of the meteorological data, which is controlling the isotopic fractionation due to evaporation.

While the computed flows for scenario A are within a plausible range for the combination of surface and groundwater outflow processes (i.e., minimum and maximum equivalent water level variations of 0.13 m d^{-1} and 0.29 m d^{-1}), scenario B yielded less realistic results (i.e., minimum and maximum equivalent water level variations of 0.004 m d^{-1} and 1.0 m d^{-1}). As mentioned above, scenario B was constrained at $\delta^{18}O \approx -11.6$‰ and $\delta^{2}H \approx -80$‰ in late April (Fig. 6), based on a surface water sample which was taken during a temporary decreasing water level period (Fig. 3) and is thus likely less representative of the overall lake's dynamic compared to scenario A. This is demonstrating the limit of the approach and that it is important to correctly constrain the model during the flood events in order to perform precise estimations of the water balance.

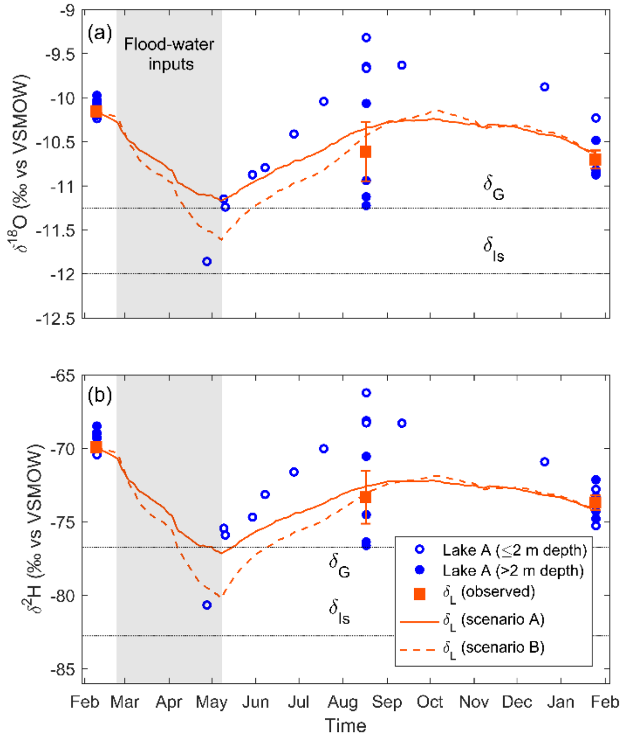

Figure 6. Observed and modelled depth-average isotopic composition of the lake (δ_L) for $\delta^{18}O$ (a) and δ^2H (b) from February 9, 2017 to January 25, 2018. Two scenarios, namely A (solid line) and B (dashed line), are modeled. The grey shaded area corresponds to the flood-water input period. The error bars correspond to the standard error on the samples for each campaign.

The water mass balance of Lake A from February 9, 2017 to January 25, 2018 is summarized in Table 2 for both scenarios. The difference between the total inputs and total outputs corresponds to the lake volume difference (1.48 x 10^5 m^3) between the start and the end of the model run. Groundwater inputs (I_G) and surface water (I_S) account for 71 % and 28 % of the total water inputs to the lake for scenario A, respectively. While I_s are twice as important for scenario B, it is only accounting for 39% (+11%) of the total inputs and the I_G are 60% (-11%). It thus appears that the annual dynamic of Lake A is dominated by groundwater inputs for both scenarios, despite the intensity of the flood event. In fact, for scenarios A and B, the mean flushing time (t_f), the ratio of the lake volume to the mean total inputs (I), is similar (i.e., 97 days and 66 days). Precipitations are contributing to 1% of the total annual inputs and evaporation only accounts for 2% of the total annual outputs. Although the establishment of a hydraulic connection between Lake DM and Lake A is a recurring yearly hydrological process, it is important to note that the magnitude and duration of the flooding event of 2017 was particularly important and, thus, had a greater impact on the dynamic of Lake A in comparison to other years.

Table 2. Water mass balance of Lake A for scenario A and B. The difference between the total inputs and total outputs corresponds to the lake volume difference over the study period. Precipitations (P), surface water inflow (I_S) and groundwater inflow (I_G) total the total inputs. Evaporation (E) and surface water and groundwater outflow (Q) total the outputs. The mean flushing time (t_f) is the ratio of the lake volume to the mean total inputs (I).

Scenario	Inputs (x 10^6 m^3)			Total I	Outputs (x 10^6 m^3)		Total Q	t_f
	P	I_S	I_G	(x 10^6 m^3)	E	Q	(x 10^6 m^3)	(days)
A	0.2	4.8	12.2	17.3	0.4	16.8	17.2	97
B	0.2	10.0	15.1	25.3	0.4	24.8	25.2	66
Difference	0.0	5.1	2.9	8.0	0.0	8.0	8.0	-31
	(0%)	(+107%)	(+24%)	(+46%)	(0%)	(+48%)	(+47%)	(-32%)

4.3.2 Sensitivity analysis

A sensitivity analysis was conducted on the input variables of the isotopic mass balance model. For each parameter, we tested two scenarios which delimit the uncertainty for each parameter. First, we tested the sensitivity of the model for V + 3 % and V – 8 % (i.e., estimated with slopes of 30° and 20°). Concerning δ_{Is} and δ_G, the model was tested for ± 0.5 ‰ for $\delta^{18}O$ and ± 4 ‰ for δ^2H, assuming they would both evolve along the LMWL (see Fig. 3). Then, we assessed for the sensitivity of the model to δ_A, by fixing the seasonality factor k at 0.5 and 0.9. Evaporation was computed with ± 20%, whereas the meteorological parameters (i.e., RH, T_{air}, U, P and Rs) were tested for ± 10%. As E and δ_A are dependent on the water surface temperature, we also tested the sensitivity of the model when considering that T is equal to the daily mean air temperature (T_{air}). Finally, we tested for the uncertainties concerning the definition of the LMWL. For the reference scenario, the LMWL was estimated using an ordinary least square regression (OLSR). For the sensitivity analysis, we estimated the LMWL via a precipitation amount weighted least square regression (PWLSR), which was developed by Hughes and Crawford (2012). By doing so, recalculation of δ_{Is}, δ_G was needed, as they were both assumed to plot on the LMWL (see Sect. 4.2).

The results of this sensitivity analysis are listed in Table D1 and Table D2 (Appendix D) for scenarios A and B. Overall, the model was found to be highly sensitive to the uncertainties associated with δ_{Is}, δ_G and E and less importantly to δ_A and T. A negligible to slight change on the modelled δ_L was found when considering the uncertainties for V, RH, T_{air}, U, P and Rs. As expected, the value of δ_{Is} is affecting the modelled δ_L exclusively during springtime (i.e., the period of hydraulic connection with Lake DM). Similarly, the values of δ_G and E particularly influence the modelled δ_L from late summer to early winter. This is due to the fact that Q and E are the dominant fluxes during this period. When considering that T is equal to T_{air}, despite the significantly different maximum and minimum values for Q, the mean Q was relatively similar to the reference scenario and only a small change for t_f was found. Finally, the model is highly sensitive to the uncertainties associated with the LMWL, as a translation of the LMWL implies an enrichment or depletion of both the δ_{Is}, δ_G at the same time.

4.4 Temporal variability in the water balance partition

The water balance presented in Table 2 provides an overview of the relative importance of the hydrological processes at Lake A for the study period (i.e., February 2017 to January 2018). As the surface water inputs (as flood-water) only occurred during springtime at Lake A, it is also important to decipher the temporal variability of the water fluxes. The dependence of a lake on groundwater can be quantified via the G-Index, which is the ratio of cumulative groundwater inputs to the cumulative total inputs (Isokangas et al., 2015). Fig. 7 shows the temporal evolution of the G-Index from February 9, 2017 to January 25, 2018 for scenario A and the associated scenarios (A1 to A22) considered in the sensitivity analysis. Note that the G-Index is calculated at a daily time-step, based on the cumulative water fluxes. It is used to understand the relative importance of groundwater inputs over the studied period and does not consider the initial state of the lake. In early February, the G-Index is 100 %, because no surface water inputs (I_S) or precipitation (P) had yet contributed to the water balance. During the flood-water input period (see grey shaded area), the G-Index rapidly decreased and reached 12 % on May 8, 2017 (for the reference scenario A). A gradual increase of the G-Index is then computed for the rest of the study period. On January 25, 2018, the G-Index is 71 % and is likely more representative of annual conditions. Despite the sensitivity of the model to the input parameters, all scenarios yielded similar results. The G-Index ranged from 62 % to 75 % on an annual timescale for the different scenarios. A discussion concerning the impact of potential surface water bank storage on the evolution of the G-Index is provided in Sect.5.2.

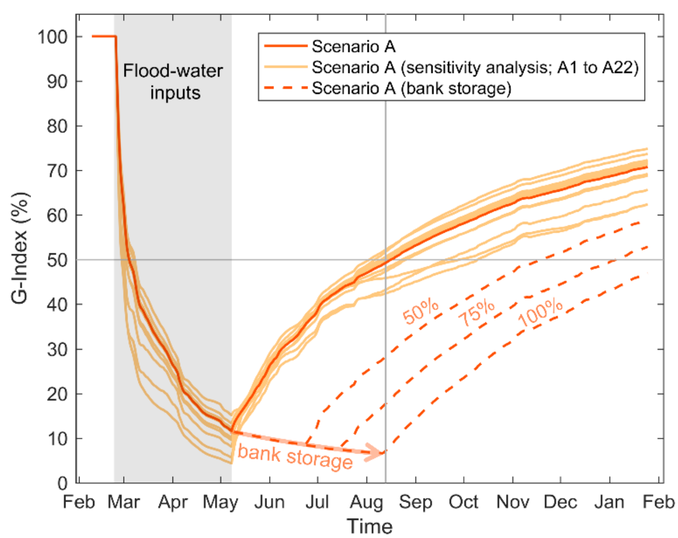

Figure 7. Temporal evolution of the G-Index from February 9, 2017 to January 25, 2018 for scenario A and the associated scenarios considered in the sensitivity analysis (i.e., A1 to A22). The grey shaded area corresponds to the flood-water input period. A hypothetical scenario is also depicted to decipher the impact of potential surface water bank storage on the evolution of the G-Index. Indeed, during the flood-water input period, the outputs (Q) from the lake can be stored in the aquifer and gradually discharge back to the lake. Conceptually, this contribution to the lake can be considered as surface water inputs (I_s), rather than groundwater inputs (I_G). Hence, G-Index is corrected for surface water bank storage considering that 50%, 75% or 100% of the Q during the flood-water input period returns to the lake as Is (dashed lines).

5. Discussion

5.1 Importance of bank storage discharge on the water balance partition

The developed isotopic mass balance model yielded significant flood-water inputs during springtime to best-fit the observed δ_L. The total flood-water volume summed to 4.82 x 10^6 m^3 (for scenario A), which is nearly equal to the lake initial volume (i.e., 4.70 x 10^6 m^3). Similar results were obtained by (Falcone, 2007) who studied the hydrological processes influencing the water balance of lakes in the Peace-Athabasca Delta, Alberta (Canada) using water isotope tracers. They reported that a springtime freshet (in 2003) did replenish the flooded lakes from 68% to >100% (88% in average).

As mentioned in Sect. 2.2, it was conceptualized that the high surface water elevation of Lake A during springtime resulted in hydraulic gradients that forced lake water to infiltrate into the aquifer and induce local recharge (see Fig. 2). An important volume of flood-derived water could thus be stored in the aquifer during the increasing water level period and eventually discharged back to the lake as its water level decreased. Hence, the groundwater inputs to Lake A following the flooding event were likely corresponding to flood-derived surface water originating from Lake DM. Considering these fluxes as surface water inputs (I_S), rather than groundwater inputs (I_G) would alter the temporal evolution of the G-Index. Such consideration is noteworthy to correctly depict the importance of flood-water inputs in the water balance partition.

A hypothetical scenario is depicted in Fig. 7 to decipher the impact of potential surface water bank storage on the evolution of the G-Index. Assuming that all outputs from the lake during the flood-water input period did eventually discharge back to the lake, the flood-water inputs would contribute to the lake water balance until early August (Fig. 7). In this hypothetical scenario, the surface water contribution to the lake would increase by 85% (due to bank storage), and prolongating the duration of the low G-index period until mid-August (Fig. 7). Lake A would thus be dependent on flood-derived water during a 3-month period after the flooding event.

Note that part of the flood-driven groundwater could have been abstracted by the pumping wells at the adjacent bank filtration site or discharged to Lake B (see the <100% scenarios in Fig. 7). In reality, the potential for flood-water bank storage is likely less important than the depicted hypothetical scenario (see the <100% scenarios in Fig. 7). Nevertheless, this hypothetical scenario illustrates the importance of considering flood-water bank storage when assessing water balances, especially as the magnitude and frequency of floods are likely to be more important in the future (Aissia et al., 2012).

5.2 Resilience of lakes to surface water and groundwater changes

Resilience of a system has been defined as its capacity to cope with perturbations (i.e., internal and/or external changes) while maintaining its state (Cumming et al., 2005). In the case of a lake, perturbations can manifest as a change in the water quantity and quality contributing to the water balance. According to Arnoux et al. (2017a), the impact of a perturbation to a lake is not only dependent on the relative importance of water budget fluxes, but also on the residence time of water in the lake. Thus, they proposed an interpretation framework which relates the response time of a lake to changes in groundwater and/or surface water quantity and/or quality thereby linking the G-Index with t_f (Fig. 8). They depict a general case, applicable to surface water pollutions in general, regardless of reactivity or fate of contaminants. Hence, care should be taken when interpreting the sensitivity to specific contaminants which are subject to attenuation processes, such as degradation and sorption.

In their study, Arnoux et al. (2017a) assessed the resilience of kettle lakes (n = 20) located in southern Quebec (Canada), in similar morpho-climatic contexts to Lake A. The surveyed lakes were found to be characterized by a wide range of conditions; from sensitive to surface water changes (i.e., G-Index < 50% and t_f>5 years) to highly sensitive to groundwater changes (i.e., G-Index>50% and t_f<1 year). This is explained by the variability of the hydrogeological contexts, resulting in variations in importance of groundwater contributions and a range of mean flushing time of lakes (see grey arrow in Fig. 8). The majority of the lakes (i.e., 50%) were found to be characterized by intermediate conditions (G-Index > 50% and 5<t_f< 1 years) and, thus, were classified as being relatively resilient to both surface and groundwater changes.

Concerning Lake A, all studied scenarios (i.e., reference scenarios A and the sensitivity analysis) yielded values for G-Index>50% and t_f<1 year, i.e., highly sensitive to groundwater changes, but resilient to surface water pollution. Nevertheless, it was shown that bank recharge, storage and discharge to lakes is crucial to correctly represent the G-Index by accounting for the origin of water fluxes (Fig.7; Sect. 5.1). While bank storage impacts the G-Index, the total water inputs (and the t_f) remain unchanged (see orange arrow in Fig. 8). Therefore, the studied lake thus receives a reduced groundwater contribution relatively to the initial estimated apportionment when not accounting for bank storage, while it benefits from having a rapid flushing time. This implies that flood-affected lakes are more likely to be characterized by an intermediate condition and, thus, are relatively resilient to both surface water and groundwater quantity and quality changes. The geochemical data (Sect. 4.2) is in accordance with this interpretation. Indeed, a low-mineralization and Ca-HCO_3 water type at Lake A is coherent with the significant flood-water contributions (to the lake and aquifer). In comparison, the neighboring lake (i.e., Lake B) does not undergo yearly recurrent flooding and was shown to be more mineralized with a Na-Cl water type, likely originating from road-salt contamination of regional groundwater (Pazouki et al., 2016). Biehler et al. (2020) similarly reported hydrological control on the geochemistry of a shallow aquifer in an hyporheic zone, where river stage influenced the mixing ratio between river water and the deeper aquifer.

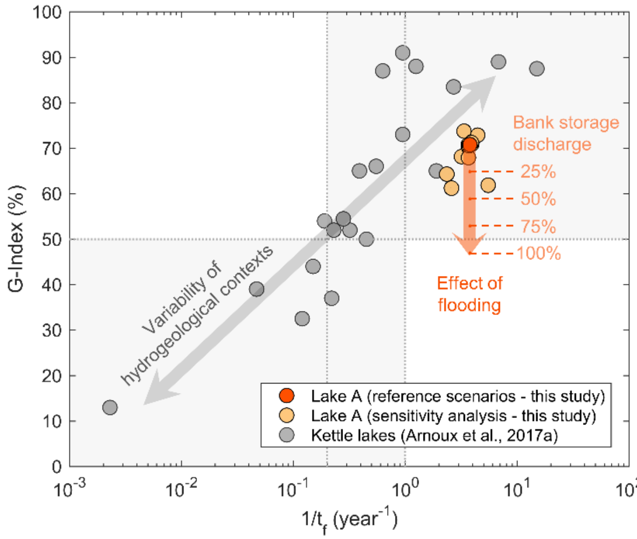

Figure 8. Resilience of lakes to groundwater quantity and quality changes for Lake A (this study) and kettle lakes (Arnoux et al., 2017a) in southern Quebec (Canada). G-Index is the ratio of groundwater inputs to total inputs and t_f is the mean flushing time. This representation is adapted from Arnoux et al. (2017a).

Considering the above, it is possible to speculate about the potential future impacts of climate change on Lake A. Globally, future meteorological scenarios are predicting changes in precipitation and climate extremes, including floods and droughts (Salinger, 2005). Studies concerning the hydrological response to future climate scenarios in Quebec, Canada have reported expected increases in water levels (Roy et al., 2001), earlier spring peak flows and overall increases in discharge (Dibike and Coulibaly, 2005) with the exception of summertime when discharge is expected to decrease (Minville et al., 2008). These hydrological responses could result in floods of longer duration and higher intensity (Aissia et al., 2012) and with more pronounced droughts (Wheaton et al., 2007). Such changes could directly affect the quality of Lake A. If flooding becomes more prevalent, enhanced flood-water input to Lake A would likely occur. In this case, the surface water inputs from floods would buffer the sensitivity of Lake A to groundwater quality changes originating from its watershed. On the other hand, if floods become less important and/or less frequent, we can expect that the water quality of Lake A would be more dependent on regional groundwater quality. In such a case, the geochemistry of Lake A could potentially shift towards that of Lake B, and an increase of the salinity and in the concentration of Na^+, Ca^{2+}, SO_4^{2+} and Cl^- would be expected for Lake A.

5.3 Implications for water management

Water budget assessments at natural lakes can serve as a tool for quantifying local human impacts (i.e., land use changes and climate changes) on the water cycle (Arnoux et al., 2017a). Based on the results of this study, it becomes apparent that water budget assessments at artificial lakes (such as Lake A) can also contribute to track human impacts on the water cycle. If repeated at a specific lake over time, such an approach will serve to document changes in groundwater and surface water apportionment and can help to detect changes in groundwater availability locally, and impacts on a local water supply utility.

As the response time of a lake to changes is controlled by its flushing time, the temporal evolution of the G-Index will manifest at various rates. Indeed, lakes with different t_f would reflect changes at different timescales. For instance, lakes with $t_f > 5$ yr would be expected to respond to decadal changes, while lakes with $t_f < 5$ yr would track annual or interannual variability. By analogy, we might postulate that it would be informative to study lakes with rapid response times (i.e., $t_f < 1$ yr), as they will act as precursors of the evolution of nearby surface water bodies characterized by longer flushing times.

As demonstrated, isotopic approaches may be efficiently employed to solve water budget unknowns as the method can be performed at low-cost and requires limited sampling and monitoring efforts for flood-affected environments which may be difficult or dangerous to monitor using traditional approaches. To enhance the effectiveness of our approach, the sampling strategy may potentially be improved. Firstly, surface water sampling for isotopic analyses is recommended during turnover periods (i.e., springtime and autumn) and should be combined with depth-resolved measurements of physico-chemical parameters to confirm the vertical homogeneity or stratification. Secondly, for long-duration flood events, monitoring of potential evolution in flood-water isotopic signatures could help to improve the accuracy and realism of the model.

6 Conclusions

In this study, we demonstrated application of isotopic mass balance to flood-affected lakes. A volume-dependent transient isotopic mass balance model was developed and applied to a flood-affected lake in an ungauged basin in southern Quebec (Canada). This allowed for better understanding of the resilience of a flood-affected lake to changes in the surface/groundwater water balance partition, to understand the role of flood-water, and to predict resilience of groundwater quantity and quality for a local water supply. A yearly recurrent hydraulic connection allows for flood-water inputs from a large watershed to the study lake during springtime. Quantification of flood-water inputs was accomplished by adjusting minimum and maximum values for surface water and groundwater outflows from the lake to best-fit the observed depth-average lake isotopic compositions. Given the contrasting isotopic signature of the flood water, the isotopic mass balance model was effectively applied at the study site. We anticipate that the isotopic framework is likely to be transferable to other lake systems subject to periodic flooding including lowland lakes fed by mountain flood-waters, river deltas, wadis, or nival (snowmelt-dominated) regimes, the latter of which dominates the high latitude and high altitude cold-regions including much of the Canadian landmass.

The isotopic mass balance model revealed that groundwater and surface water inputs account for 71 % and 28 %, respectively, of the total annual water inputs to Lake A, which demonstrates a dominance of groundwater inputs in the annual water budget. To test the sensitivity, representativeness and resilience of the model, several model scenarios were evaluated to account for uncertainty in important input variables. Despite sensitivity to some variables, all model scenarios converged on the result that Lake A is likely to be highly sensitive to groundwater quantity and quality changes. However, there is a likelihood that the sensitivity to groundwater changes is somewhat reduced from April to August, when important surface water inputs originating from Lake DM dominate the water balance. During springtime, we estimate flood-water inputs from Lake DM to Lake A occurred at a mean rate of 6.61×10^4 m^3 d^{-1}, with a total flood-water volume of 4.82×10^6 m^3 (i.e., roughly equivalent to the initial lake's volume). Meanwhile, the high water level during springtime induced a hydraulic gradient which forced lake water to infiltrate into the aquifer and resulted in local flood-water recharge. An important volume of flood-derived surface water could thus be stored within the aquifer in spring which was subsequently discharged back to the lake during summertime, as its surface elevation decreased. This suggests that the surface water fluxes between Lake DM and Lake A not only have an impact on the dynamics of Lake A during springtime, but also significantly influence the annual water budget. This finding provides a basis for postulating the impact of climate change on the water quality of Lake A. If the importance of floods increases, more flood-water inputs to Lake A can be expected during springtime, causing increased recharge. In this case, the surface water inputs from floods would increase the resilience of flood-affected lakes to groundwater quantity and quality changes at the watershed scale. On the other hand, if floods become less important and/or less frequent, we can expect that the water quality of flood-affected lakes become more dependent on regional groundwater quality. From a global perspective, performing water balance assessments at lakes with rapid flushing time (< 1 year) can help at predicting the evolution of other surface water resources with longer flushing time in their vicinity and, therefore, is useful for establishing regional-scale management strategies for maintaining lake water quality.

Appendix A

Computation of isotope mass balance parameters

The parameter f(u), for the estimation of E (Eq. (4)), is calculated according to the area-dependent expression described by McJannet et al. (2012):

$$f(u) = (2.36 + 1.67u)A^{-0.05} \tag{5}$$

where u is the wind speed (m s^{-1}) measured at 2 m above the ground and A is the area (m^{2}) of the lake. Note that Eq. (5) was developed for land-based meteorological data.

The isotopic composition of the evaporating moisture (δ_E) is estimated based on the Craig and Gordon (1965) model and, as described by Gonfiantini (1986), is:

$$\delta_E = \frac{\frac{(\delta_L - \varepsilon^+)}{\alpha^+} - h\delta_A - \varepsilon_K}{1 - h + 10^{-3}\varepsilon_K} \ (‰) \tag{6}$$

where h is the relative humidity normalized to water surface temperature (in decimal fraction), δ_A is the isotopic composition of atmospheric moisture (described later on), ε^+ is the equilibrium isotopic separation and ε_K is the kinetic isotopic separation, with $\varepsilon^+=(\alpha^+-1)10^3$ and $\varepsilon_K=\theta*C_K(1-h)$. α^+ is the equilibrium isotopic fractionation, θ is a transport resistance parameter and C_K is the ratio of molecular diffusivities of the heavy and light molecules. θ is expected to be close to 1 for small lakes (Gibson et al., 2015) and C_K is typically fixed at 14.2 ‰ and 12.5 ‰ for $\delta^{18}O$ and δ^2H respectively in lake studies as these values represent fully turbulent wind conditions (Horita et al., 2008). Experimental values for α^+ were used (Horita and Wesolowski, 1994):

$$\alpha^+(^{18}O) = \exp\left[-\frac{7.685}{10^3} + \frac{6.7123}{(T+273.15)} - \frac{16666.4}{(T+273.15)^2} + \frac{350410}{(T+273.15)^3}\right] \tag{7a}$$

$$\alpha^+(^{2}H) = \exp\left[1158.8\left(\frac{(T+273.15)^3}{10^{12}}\right) + 1620.1\left(\frac{(T+273.15)^2}{10^9}\right) + 794.84\left(\frac{(T+273.15)}{10^6}\right) - \frac{161.04}{10^3} + \frac{2999200}{(T+273.15)^3}\right] \tag{7b}$$

where T is the water surface temperature (°C), which was estimated according to the equilibrium method as described by de Bruin (1982) (see Appendix C).

The parameters m and δ_s, for the computation of δ_L (Eq. (3)), are calculated as (Gibson, 2002):

$$m = \frac{\left(h - 10^{-3}\cdot\left(\varepsilon_K + \frac{\varepsilon^+}{\alpha^+}\right)\right)}{(1 - h + 10^{-3}\cdot\varepsilon_K)} \tag{8}$$

$$\delta_S = \frac{\delta_I + mX\delta^*}{1 + mX} \tag{9}$$

where, and δ^* is the limiting isotopic composition that the lake would approach as V → 0 and is calculated as:

$$\delta^* = \left(h\delta_A + \varepsilon_K + \frac{\varepsilon^+}{\alpha^+}\right) \Big/ \left(h - 10^{-3}\cdot\left(\varepsilon_K + \frac{\varepsilon^+}{\alpha^+}\right)\right) \tag{10}$$

The isotopic composition of atmospheric moisture (δ_A) is estimated using the partial equilibrium model of Gibson et al. (2015):

$$\delta_A = \frac{\delta_P - k\varepsilon^+}{1 + 10^{-3} \cdot k\varepsilon^+} \qquad (11)$$

where δ_P is the isotopic composition of precipitation and k is a seasonality factor, fixed to 0.5 in this study. The k value (ranging from 0.5 to 1) is selected to provide a best-fit between the measured and modelled local evaporation line. In Eq. (13), δ_P and monthly exchange parameters (ε^+, α^+ and ε_K) are evaporation flux-weighted based on daily evaporation records.

Appendix B

Comparison of the evaporative fluxes (E) estimations

See Fig. B1

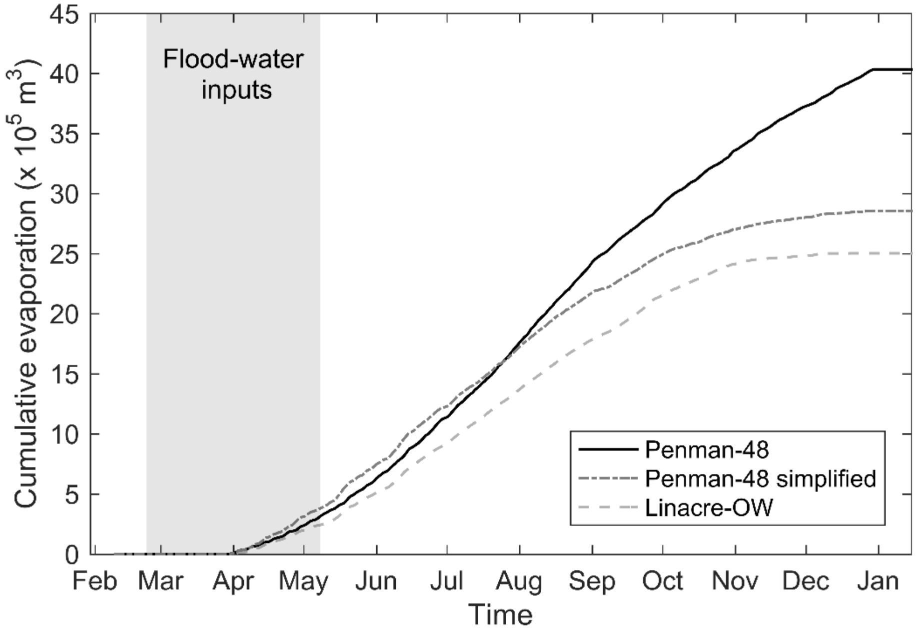

Figure B1. Cumulative evaporative fluxes from Lake A via the Penman-48, Penman-48 simplified method (Valiantzas, 2006) and Linacre-OW (Linacre, 1977) methods.

Appendix C

Estimation of the water surface temperature based on the equilibrium method (de Bruin, 1982)

The water surface temperature (T) was estimated via the equilibrium method presented by de Bruin (1982), because no continuous measurements were available. This model is based on the assumption of a well-mixed surface body and was developed from standard land-based weather data. It was tested on two adjacent reservoirs in the Netherlands with average depths of 5 m and 15 m, respectively. Similarly to de Bruin (1982), we used the 10-day mean values, because we are interested in the annual variations of the water temperature. Moreover, the 10-day mean values were found to better simulate the observed water surface temperature. Differences between the observed and modelled water temperature is typically ≤1 °C, except in July and December where discrepancies up to 5 °C were observed (Fig. C1). This is likely because Lake A develops a thermal stratification over summertime and in wintertime. Potential uncertainties in isotopic mass balance models due to stratification in lakes up to 35 m were previously described and discussed by Gibson et al. (2017) and (Gibson et al., 2019). They reported that sampling methods and lake stratification can lead to volume-dependent bias in the water balance partition. In this study, not accounting fully for thermal stratification will lead to overestimation of evaporation fluxes, and groundwater exchange will be potentially underestimated.

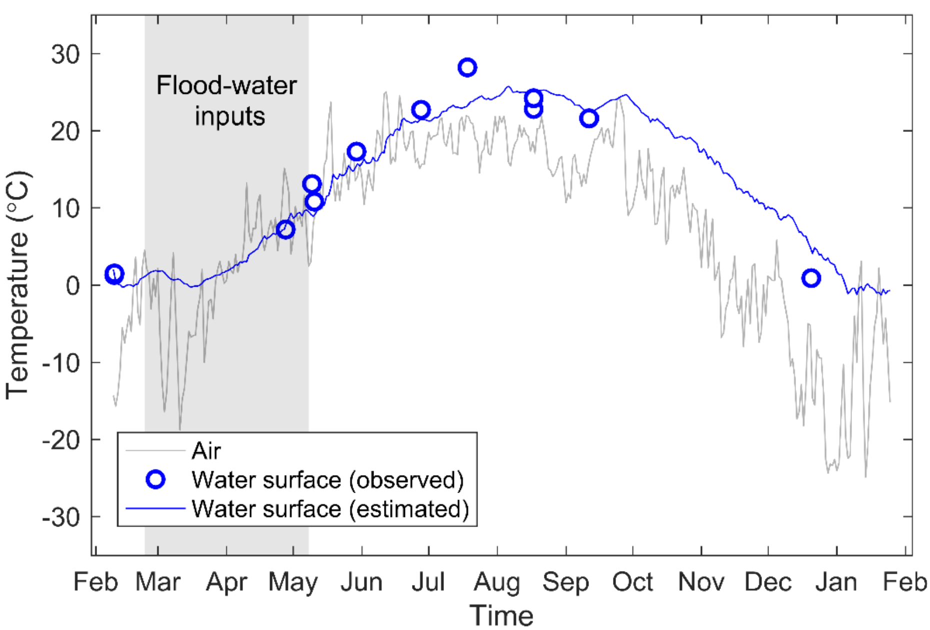

Figure C1. Temporal evolution of air temperature and observed and estimated water surface temperatures at Lake A. Water surface temperature estimations were computed according to the equilibrium method described by de Bruin (1982).

Appendix D

Results of the sensitivity analysis for reference scenarios A and B

See Table D1 and Table D2.

Table D1. Sensitivity analysis on the input parameters of the isotopic mass balance model. Q is the output flux from Lake A, I the input flux and t_f the mean flushing time.

	Scenario	Maximum Q	Minimum Q	Mean Q		Mean I		t_f
				Flooding	Annual	Flooding	Annual	
		(x 10^4 m^3/day)	(x 10^4 m^3/day)	(x 10^4 m^3/day)		(x 10^4 m^3/day)		(days)
A	Reference	8.0	3.7	5.64	4.77	6.61	4.86	97
A01	V + 3% (slope 30°)	8.0	3.7	5.64	4.77	6.61	4.86	100
A02	V - 8% (slope 20°)	7.8	3.7	5.55	4.72	6.51	4.81	93
A03	δ_{Is} ^{18}O + 0.5 ‰ δ_{Is} ^{2}H + 4.06 ‰	25.0	1.0	11.82	6.99	12.79	7.08	66
A04	δ_{Is} ^{18}O - 0.5 ‰ δ_{Is} ^{2}H - 4.06 ‰	4.3	4.2	4.25	4.22	5.21	4.31	109
A05	δ_{G} ^{18}O + 0.5 ‰ δ_{G} ^{2}H + 4.06 ‰	Not possible to fit data						
A06	δ_{G} ^{18}O - 0.5 ‰ δ_{G} ^{2}H - 4.06 ‰	10.0	1.0	5.06	3.25	6.02	3.34	141
A07	δ_A minimum	Not possible to fit data						
A08	δ_A maximum	8.0	4.0	5.80	5.00	6.77	5.09	92
A09	E + 20%	8.0	4.8	6.24	5.60	7.22	5.72	82
A10	E - 20%	8.0	2.7	5.09	4.02	6.05	4.09	115
A11	RH + 10%	Negligible change						
A12	RH - 10%							
A13	T_{air} + 10%	8.0	3.9	5.75	4.92	6.71	5.01	94
A14	T_{air} - 10%	8.0	3.5	5.53	4.62	6.50	4.71	100
A15	U + 10%	8.0	3.9	5.75	4.92	6.72	5.01	94
A16	U - 10%	8.0	3.6	5.58	4.70	6.55	4.78	98
A17	P + 10%	Negligible change						
A18	P - 10%							
A19	T = T_{air}	10.0	2.9	6.10	4.67	7.07	4.73	100
A20	Rs + 10%	8.0	3.9	5.75	4.92	6.72	5.02	94
A21	Rs - 10%	8.0	3.6	5.58	4.70	6.55	4.78	98
A22	LMWL (PWLSR method)	7.0	1.6	4.04	2.95	5.00	3.03	155

Table D2. Sensitivity analysis on the input parameters of the isotopic mass balance model for the reference scenario B. Q is the output flux from Lake A, I the input flux and t_f the mean flushing time.

Scenario		Maximum Q (x 10^4 m^3/day)	Minimum Q (m^3/day)	Mean Q (x 10^4 m^3/day)		Mean I (x 10^4 m^3/day)		t_f (days)
				Flooding	Annual	Flooding	Annual	
B	Reference	28.0	1.0E+03	12.68	7.07	13.65	7.16	66
B01	V + 3% (slope 30°)	28.0	1.0E+01	12.63	6.99	13.59	7.07	69
B02	V - 8% (slope 20°)	26.0	1.0E+01	11.73	6.49	12.69	6.57	68
B03	δ_{Is} ^{18}O + 0.5 ‰ δ_{Is} ^{2}H + 4.06 ‰	Not possible to fit data						
B04	δ_{Is} ^{18}O - 0.5 ‰ δ_{Is} ^{2}H - 4.06 ‰	12.0	2.5E+04	6.78	4.87	7.75	4.95	95
B05	δ_{G} ^{18}O + 0.5 ‰ δ_{G} ^{2}H + 4.06 ‰	Not possible to fit data						
B06	δ_{G} ^{18}O - 0.5 ‰ δ_{G} ^{2}H - 4.06 ‰	Not possible to fit data						
B07	δ_A minimum	26.0	1.0E+01	11.73	6.49	12.69	6.57	72
B08	δ_A maximum	Negligible change						
B09	E + 20%	28.0	1.0E+04	13.18	7.74	14.15	7.84	60
B10	E - 20%	27.0	1.0E+01	12.18	6.74	13.13	6.80	69
B11	RH + 10%	Negligible change						
B12	RH - 10%							
B13	T_{air} + 10%	Negligible change						
B14	T_{air} - 10%							
B15	U + 10%	28.0	2.0E+03	12.74	7.14	13.70	7.23	65
B16	U - 10%	28.0	1.0E+01	12.63	6.99	13.59	7.08	66
B17	P + 10%	Negligible change						
B18	P - 10%							
B19	T = T_{air}	28.0	1.0E+01	12.63	6.99	13.60	7.05	67
B20	Rs + 10%	28.0	3.0E+03	12.79	7.22	13.76	7.31	64
B21	Rs - 10%	28.0	1.0E+01	12.63	6.99	13.59	7.07	67
B22	LMWL (PWLSR method)	16.0	1.0E+01	7.22	4.00	8.18	4.08	115

Author contribution

JMD: Conceptualization, Data curation, Investigation, Methodology, Visualization, Roles/Writing - original draft. FB: Conceptualization, Methodology, Supervision, Writing - review & editing. PB: Conceptualization, Funding acquisition, Project administration, Supervision, Writing - review & editing. JG: Methodology, Writing - review & editing.

Competing interests

The authors declare that they have no conflict of interest.

Acknowledgements

This research was funded by NSERC, grant numbers CRSNG-RDCPJ: 523095-17 and CRSNG-RGPIN-2016-06780.The authors are grateful to the Town and G. Rybicki to allow access and water sampling on their property. Thanks to the students (M. Patenaude, T. Crouzal, R.-A. Farley, just to name a few) who participated in the fieldwork. We also gratefully acknowledge J.-F. Helie and M. Tcaci from Geotop-UQAM and M. Leduc and J. Leroy from the Laboratoire de géochimie de Polytechnique Montréal.

References

Ageos: Drinking water supply: Application for an authorization under Section 31 of Groundwater Catchment Regulation: Hydrogeological expert report, AGEOS, Brossard, QC, Canada2010-723, volume 1 de 2, 2010.

Ageos: Drinking water supply: Monitoring of piezometric fluctuations in the water table and lake levels: Period from April 27, 2012 to December 17, 2015: Annual Report 2015, AGEOS, Brossard, QC, Canada, 42, 2016.

Aissia, M. A. B., Chebana, F., Ouarda, T. B. M. J., Roy, L., Desrochers, G., Chartier, I., and Robichaud, É.: Multivariate analysis of flood characteristics in a climate change context of the watershed of the Baskatong reservoir, Province of Québec, Canada, Hydrological Processes, 26, 130-142, 10.1002/hyp.8117, 2012.

Arnoux, M., Barbecot, F., Gibert-Brunet, E., Gibson, J., Rosa, E., Noret, A., and Monvoisin, G.: Geochemical and isotopic mass balances of kettle lakes in southern Quebec (Canada) as tools to document variations in groundwater quantity and quality, Environmental Earth Sciences, 76, 106, 10.1007/s12665-017-6410-6, 2017a.

Arnoux, M., Gibert-Brunet, E., Barbecot, F., Guillon, S., Gibson, J., and Noret, A.: Interactions between groundwater and seasonally ice-covered lakes: Using water stable isotopes and radon-222 multilayer mass balance models, Hydrological Processes, 31, 2566-2581, 10.1002/hyp.11206, 2017b.

Barbecot, F., Larocque, M., and Horoi, V. Research infrastructure on groundwater recharge, [Isotopic composition of precipitation at St-Bruno, QC Canada], 2019.

Biehler, A., Chaillou, G., Buffin-Bélanger, T., and Baudron, P.: Hydrological connectivity in the aquifer–river continuum: impact of river stages on the geochemistry of groundwater floodplains, Journal of Hydrology, 125379, 10.1016/j.jhydrol.2020.125379, 2020.

Bocanegra, E., Quiroz Londoño, O. M., Martínez, D. E., and Romanelli, A.: Quantification of the water balance and hydrogeological processes of groundwater–lake interactions in the Pampa Plain, Argentina, Environmental Earth Sciences, 68, 2347-2357, 10.1007/s12665-012-1916-4, 2013.

Brock, B. E., Wolfe, B. B., and Edwards, T. W. D.: Characterizing the Hydrology of Shallow Floodplain Lakes in the Slave River Delta, NWT, Canada, Using Water Isotope Tracers, Arctic, Antarctic, and Alpine Research, 39, 388-401, 10.1657/1523-0430(06-026)[BROCK]2.0.CO;2, 2007.

Centre d'Expertise Hydrique du Québec. Délimitation des bassins versants correspondant aux stations hydrométriques ouvertes et fermées, Retrieved from: https://www.cehq.gouv.qc.ca/hydrometrie/index.htm, 2019.

Centre d'Expertise Hydrique du Québec. Niveau d'eau à la station 043108 (Lac des Deux Montagnes), Retrieved from: http://cehq.gouv.qc.ca/depot/historique_donnees_instantanees/043108_N_2017.txt, 2020.

Clark, I.: Groundwater Geochemistry and Isotopes, Boca Raton, FL, 2015.

Craig, H., and Gordon, L. I.: Deuterium and oxygen 18 variations in the ocean and the marine atmosphere, in: Stable isotopes in oceanographic studies and paleotemperatures, edited by: Tongiorgi, E., Lab. Geologia Nucleare, Pisa, 9-130, 1965.

Cumming, G. S., Barnes, G., Perz, S., Schmink, M., Sieving, K. E., Southworth, J., Binford, M., Holt, R. D., Stickler, C., and Van Holt, T.: An Exploratory Framework for the Empirical Measurement of Resilience, Ecosystems, 8, 975-987, 10.1007/s10021-005-0129-z, 2005.

Cunha, D. G. F., Sabogal-Paz, L. P., and Dodds, W. K.: Land use influence on raw surface water quality and treatment costs for drinking supply in São Paulo State (Brazil), Ecological Engineering, 94, 516-524, 10.1016/j.ecoleng.2016.06.063, 2016.

de Bruin, H. A. R.: Temperature and energy balance of a water reservoir determined from standard weather data of a land station, Journal of Hydrology, 59, 261-274, 10.1016/0022-1694(82)90091-9, 1982.

Delpla, I., Jung, A. V., Baures, E., Clement, M., and Thomas, O.: Impacts of climate change on surface water quality in relation to drinking water production, Environment International, 35, 1225-1233, 10.1016/j.envint.2009.07.001, 2009.

Dibike, Y. B., and Coulibaly, P.: Hydrologic impact of climate change in the Saguenay watershed: comparison of downscaling methods and hydrologic models, Journal of Hydrology, 307, 145-163, 10.1016/j.jhydrol.2004.10.012, 2005.

Edwards, T. W. D., Wolfe, B. B., Gibson, J. J., and Hammarlund, D.: Use of water isotope tracers in high latitude hydrology and paleohydrology, in: Long-term environmental change in Arctic and Antarctic Lakes, developments in paleoenvironmental research, edited by: Pienitz, R., Douglas, M., and Smol, J. P., Springer, Dordrecht, Netherlands, 187-207, 2004.

Falcone, M.: Assessing hydrological processes controlling the water balance of lakes in the Peace-Athabasca Delta, Alberta, Canada using water isotope tracers, UWSpace, 2007.

Gibson, J. J., Edwards, T. W. D., Bursey, G. G., and Prowse, T. D.: Estimating Evaporation Using Stable Isotopes: Quantitative Results and Sensitivity Analysis for Two Catchments in Northern Canada: Paper presented at the 9th Northern Res. Basin Symposium/Workshop (Whitehorse/Dawson/Inuvik, Canada - August 1992), Hydrology Research, 24, 79-94, 10.2166/nh.1993.0015, 1993.

Gibson, J. J.: Short-term evaporation and water budget comparisons in shallow Arctic lakes using non-steady isotope mass balance, Journal of Hydrology, 264, 242-261, 10.1016/S0022-1694(02)00091-4, 2002.

Gibson, J. J., Birks, S. J., and Yi, Y.: Stable isotope mass balance of lakes: a contemporary perspective, Quaternary Science Reviews, 131, 316-328, 10.1016/j.quascirev.2015.04.013, 2015.

Gibson, J. J., Birks, S. J., Yi, Y., Moncur, M. C., and McEachern, P. M.: Stable isotope mass balance of fifty lakes in central Alberta: Assessing the role of water balance parameters in determining trophic status and lake level, Journal of Hydrology: Regional Studies, 6, 13-25, 10.1016/j.ejrh.2016.01.034, 2016.

Gibson, J. J., Birks, S. J., Jeffries, D., and Yi, Y.: Regional trends in evaporation loss and water yield based on stable isotope mass balance of lakes: The Ontario Precambrian Shield surveys, Journal of Hydrology, 544, 500-510, 10.1016/j.jhydrol.2016.11.016, 2017.

Gibson, J. J., Yi, Y., and Birks, S. J.: Isotopic tracing of hydrologic drivers including permafrost thaw status for lakes across Northeastern Alberta, Canada: A 16-year, 50-lake assessment, Journal of Hydrology: Regional Studies, 26, 100643, 10.1016/j.ejrh.2019.100643, 2019.

Gonfiantini, R.: Chapter 3 - ENVIRONMENTAL ISOTOPES IN LAKE STUDIES, in: The Terrestrial Environment, B, edited by: Fritz, P., and Fontes, J. C., Elsevier, Amsterdam, 113-168, 1986.

Gran, G.: Determination of the equivalence point in potentiometric titrations. Part II, Analyst, 77, 661-671, 10.1039/AN9527700661, 1952.

Haig, H. A., Hayes, N. M., Simpson, G. L., Yi, Y., Wissel, B., Hodder, K. R., and Leavitt, P. R.: Comparison of isotopic mass balance and instrumental techniques as estimates of basin hydrology in seven connected lakes over 12 years, Journal of Hydrology X, 6, 100046, https://doi.org/10.1016/j.hydroa.2019.100046, 2020.

Herczeg, A. L., Leaney, F. W., Dighton, J. C., Lamontagne, S., Schiff, S. L., Telfer, A. L., and English, M. C.: A modern isotope record of changes in water and carbon budgets in a groundwater-fed lake: Blue Lake, South Australia, Limnology and Oceanography, 48, 2093-2105, 10.4319/lo.2003.48.6.2093, 2003.

Holtz, R. D., and Kovacs, W. D.: An Introduction to Geotechnical Engineering, Montreal, Canada, 832 pp., 1981.

Horita, J., and Wesolowski, D. J.: Liquid-vapor fractionation of oxygen and hydrogen isotopes of water from the freezing to the critical temperature, Geochimica et Cosmochimica Acta, 58, 3425-3437, 10.1016/0016-7037(94)90096-5, 1994.

Horita, J., Rozanski, K., and Cohen, S.: Isotope effects in the evaporation of water: a status report of the Craig–Gordon model, Isotopes in Environmental and Health Studies, 44, 23-49, 10.1080/10256010801887174, 2008.

Hughes, C. E., and Crawford, J.: A new precipitation weighted method for determining the meteoric water line for hydrological applications demonstrated using Australian and global GNIP data, Journal of Hydrology, 464-465, 344-351, 10.1016/j.jhydrol.2012.07.029, 2012.

IAEA/WMO. Global Network of Isotopes in Precipitation. The GNIP Database., Retrieved from: https://nucleus.iaea.org/wiser, 2018.

Isokangas, E., Rozanski, K., Rossi, P. M., Ronkanen, A. K., and Kløve, B.: Quantifying groundwater dependence of a sub-polar lake cluster in Finland using an isotope mass balance approach, Hydrol. Earth Syst. Sci., 19, 1247-1262, 10.5194/hess-19-1247-2015, 2015.

Jeppesen, E., Meerhoff, M., Davidson, T. A., Trolle, D., SondergaarD, M., Lauridsen, T. L., Beklioglu, M., Brucet Balmaña, S., Volta, P., and González-Bergonzoni, I.: Climate change impacts on lakes: an integrated ecological perspective based on a multi-faceted approach, with special focus on shallow lakes, 73, 88-111, 10.4081/jlimnol.2014.844, 2014.

Kløve, B., Ala-aho, P., Bertrand, G., Boukalova, Z., Ertürk, A., Goldscheider, N., Ilmonen, J., Karakaya, N., Kupfersberger, H., Kværner, J., Lundberg, A., Mileusnić, M., Moszczynska, A., Muotka, T., Preda, E., Rossi, P., Siergieiev, D., Šimek, J., Wachniew, P., Angheluta, V., and Widerlund, A.: Groundwater dependent ecosystems. Part I: Hydroecological status and trends, Environmental Science & Policy, 14, 770-781, 10.1016/j.envsci.2011.04.002, 2011.

Lerner, D. N., and Harris, B.: The relationship between land use and groundwater resources and quality, Land Use Policy, 26, S265-S273, 10.1016/j.landusepol.2009.09.005, 2009.

Linacre, E. T.: A simple formula for estimating evaporation rates in various climates, using temperature data alone, Agricultural Meteorology, 18, 409-424, 10.1016/0002-1571(77)90007-3, 1977.

Masse-Dufresne, J., Baudron, P., Barbecot, F., Patenaude, M., Pontoreau, C., Proteau-Bedard, F., Menou, M., Pasquier, P., Veuille, S., and Barbeau, B.: Anthropic and Meteorological Controls on the Origin and Quality of Water at a Bank Filtration Site in Canada, Water, 11, 2510, 10.3390/w11122510, 2019.

Masse-Dufresne, J., Baudron, P., Barbecot, F., Pasquier, P., and Barbeau, B.: Optimizing short time-step monitoring and management strategies using environmental tracers at flood-affected bank filtration sites, Science of The Total Environment, 750, 141429, 10.1016/j.scitotenv.2020.141429, 2020.

McJannet, D. L., Webster, I. T., and Cook, F. J.: An area-dependent wind function for estimating open water evaporation using land-based meteorological data, Environmental Modelling & Software, 31, 76-83, 10.1016/j.envsoft.2011.11.017, 2012.

Minville, M., Brissette, F., and Leconte, R.: Uncertainty of the impact of climate change on the hydrology of a nordic watershed, Journal of Hydrology, 358, 70-83, 10.1016/j.jhydrol.2008.05.033, 2008.

Mueller, H., Hamilton, D. P., and Doole, G. J.: Evaluating services and damage costs of degradation of a major lake ecosystem, Ecosystem Services, 22, 370-380, 10.1016/j.ecoser.2016.02.037, 2016.

O'Neil, J. R.: Hydrogen and oxygen isotope fractionation between ice and water, The Journal of Physical Chemistry, 72, 3683-3684, 10.1021/j100856a060, 1968.

Patenaude, M., Baudron, P., Labelle, L., and Masse-Dufresne, J.: Evaluating Bank-Filtration Occurrence in the Province of Quebec (Canada) with a GIS Approach, Water, 12, 662, 10.3390/w12030662, 2020.

Pazouki, P., Prevost, M., McQuaid, N., Barbeau, B., de Boutray, M. L., Zamyadi, A., and Dorner, S.: Breakthrough of cyanobacteria in bank filtration, Water Res, 102, 170-179, 10.1016/j.watres.2016.06.037, 2016.

Petermann, E., Gibson, J. J., Knöller, K., Pannier, T., Weiß, H., and Schubert, M.: Determination of groundwater discharge rates and water residence time of groundwater-fed lakes by stable isotopes of water (18O, 2H) and radon (222Rn) mass balances, Hydrological Processes, 32, 805-816, 10.1002/hyp.11456, 2018.

Rosa, E., Hillaire-Marcel, C., Hélie, J.-F., and Myre, A.: Processes governing the stable isotope composition of water in the St. Lawrence river system, Canada, Isotopes in Environmental and Health Studies, 52, 370-379, 10.1080/10256016.2015.1135138, 2016.

Rosen, M. R.: The Influence of Hydrology on Lacustrine Sediment Contaminant Records, in: Environmental Contaminants: Using natural archives to track sources and long-term trends of pollution, edited by: Blais, J. M., Rosen, M. R., and Smol, J. P., Springer Netherlands, Dordrecht, 5-33, 2015.

Rosenberry, D. O., Lewandowski, J., Meinikmann, K., and Nützmann, G.: Groundwater - the disregarded component in lake water and nutrient budgets. Part 1: effects of groundwater on hydrology, Hydrological Processes, 29, 2895-2921, 10.1002/hyp.10403, 2015.

Roy, L., Leconte, R., Brissette, F. P., and Marche, C.: The impact of climate change on seasonal floods of a southern Quebec River Basin, Hydrological Processes, 15, 3167-3179, 10.1002/hyp.323, 2001.

Sacks, L. A., Lee, T. M., and Swancar, A.: The suitability of a simplified isotope-balance approach to quantify transient groundwater–lake interactions over a decade with climatic extremes, Journal of Hydrology, 519, 3042-3053, 10.1016/j.jhydrol.2013.12.012, 2014.

Salinger, M. J.: Climate Variability and Change: Past, Present and Future – An Overview, Climatic Change, 70, 9-29, 10.1007/s10584-005-5936-x, 2005.

Scanlon, B. R., Reedy, R. C., Stonestrom, D. A., Prudic, D. E., and Dennehy, K. F.: Impact of land use and land cover change on groundwater recharge and quality in the southwestern US, Global Change Biology, 11, 1577-1593, 10.1111/j.1365-2486.2005.01026.x, 2005.

Schallenberg, M., de Winton, M. D., Verburg, P., Kelly, D. J., Hamill, K. D., and Hamilton, D. P.: Ecosystem services of lakes, in: Ecosystem services in New Zealand: conditions and trends. Manaaki Whenua Press, Lincoln, edited by: Dymond, J. R., Manaaki Whenua Press, Lincoln, New Zealand, 203-225, 2013.

Stets, E. G., Winter, T. C., Rosenberry, D. O., and Striegl, R. G.: Quantification of surface water and groundwater flows to open- and closed-basin lakes in a headwaters watershed using a descriptive oxygen stable isotope model, Water Resources Research, 46, 10.1029/2009WR007793, 2010.

Turner, K. W., Wolfe, B. B., and Edwards, T. W. D.: Characterizing the role of hydrological processes on lake water balances in the Old Crow Flats, Yukon Territory, Canada, using water isotope tracers, Journal of Hydrology, 386, 103-117, 10.1016/j.jhydrol.2010.03.012, 2010.

Valiantzas, J. D.: Simplified versions for the Penman evaporation equation using routine weather data, Journal of Hydrology, 331, 690-702, 10.1016/j.jhydrol.2006.06.012, 2006.

Walsh, J. R., Carpenter, S. R., and Vander Zanden, M. J.: Invasive species triggers a massive loss of ecosystem services through a trophic cascade, Proceedings of the National Academy of Sciences, 113, 4081, 10.1073/pnas.1600366113, 2016.

Wolfe, B. B., Karst-Riddoch, T. L., Hall, R. I., Edwards, T. W. D., English, M. C., Palmini, R., McGowan, S., Leavitt, P. R., and Vardy, S. R.: Classification of hydrological regimes of northern floodplain basins (Peace–Athabasca Delta, Canada) from analysis of stable isotopes (δ18O, δ2H) and water chemistry, Hydrological Processes, 21, 151-168, 10.1002/hyp.6229, 2007.

Zimmermann, U.: Determination by stable isotopes of underground inflow and outflow and evaporation of young artificial groundwater lakes, in: Isotopes in lakes studies, IAEA, Vienna, Austria, 87-94, 1979.